Effects of Insulinlike Growth Factor Binding Proteins on Insulinlike Growth Factor-I Biodistribution in Tumor-Bearing Nude Mice

Bao-Fu Sun, Hisataka Kobayashi, Nhat Le, Tae M. Yoo, Debra Drumm, Chang H. Paik, John G. McAfee, and Jorge A. Carrasquillo

Department of Nuclear Medicine, Warren G. Magnuson Clinical Center, National Institutes of Health, Bethesda, Maryland

This study evaluated the biodistribution and tumor targeting ability of radiolabeled insulinlike growth factor (IGF)-I. Because IGF binding proteins (IGFBPs) play a critical role in modulating IGF activity, the binding properties of ^{125}I-labeled IGF-I to IGFBPs were investigated in vitro and in vivo. Because a large amount of the IGF-I was catabolized in vivo, we also studied the catabolism of IGF-I by tumor cells in vitro. **Methods:** ^{125}I-labeled-IGF-I was prepared using the chloramine T method. The biodistribution of ^{125}I-labeled-IGF-I in tumor-bearing nude mice was compared between groups injected with ^{125}I-labeled IGF-I alone or coinjected with unlabeled peptide. In vitro and in vivo chromatography studies were performed to evaluate the binding profile to IGFBPs and the degree of catabolites in serum as well as urine. **Results:** Data indicated that the binding of radiolabeled IGF-I to IGFBPs in vitro was dose dependent. However, there was a difference in complex formation between the serum and the heparinized plasma. In heparinized plasma, the radioactivity shifted from a 30- to 50-kDa complex to a 150-kDa complex and to a free ligand, because the binding of heparin with IGFBPs decreased its affinity for IGF-I. In plasma prepared with acid citrate dextrose a binding pattern identical to that of serum was observed. Moreover, there was a binding difference between mouse and rat. The ^{125}I-labeled IGF-I catabolized very quickly when incubated at 37°C but not at all at 4°C. In tumor-bearing nude mice, the uptake of radioactivity in normal tissues decreased quickly, particularly in the kidneys. In mice coinjected with unlabeled carrier, the radioactivity in most normal tissues was lower and the tumor uptake higher than in the mice without carrier. **Conclusion:** These data confirm that ^{125}I-labeled IGF-I is avidly bound to IGFBPs, both in vitro and in vivo. By partially saturating this binding with unlabeled peptides, a favorable biodistribution was achieved, including faster clearance from normal tissue and higher tumor uptake, which resulted in better tumor-to-nontumor ratios. Nevertheless, the rapid catabolism and release of the radiolabel from tumor tissue result in a suboptimal targeting agent.

Key Words: insulinlike growth factor-I; insulinlike growth factor receptor; insulinlike growth factor binding proteins; endocytosis

J Nucl Med 2000; 41:318–326

The insulinlike growth factor (IGF) system has 3 components: ligands, receptors, and binding proteins. Two ligands, IGF-I and IGF-II, have been identified (*1*). Circulating IGF-I and IGF-II are produced mainly in the liver, and they act on distant targets through an endocrine pathway (*2*). Other tissues, including various tumors, also produce IGFs, but these act locally through paracrine or autocrine pathways (*3,4*). These IGFs play an important role in the physical development of humans and animals (*2,5*). They are critical also in stimulating cell growth, differentiation, and proliferation (*6–10*). Moreover, the mitogenic and tumorigenic roles of IGFs on neoplastic cells have been well documented (*11–13*).

At least 2 receptors exist for IGFs: type I IGF receptor (IGF-IR) and type II IGF receptor (IGF-IIR). These receptors are present not only in normal cell lines but also in many neoplastic cells, in which they are overexpressed (*14–17*). These membrane receptors mediate the intracellular actions of IGFs. The IGF-IR is a heterotetramer with 2 α subunits, which bind these ligands and are entirely extracellular, and 2 β subunits, which span the membrane.

To date, 6 IGF binding proteins (IGFBPs) have been cloned and their cDNA sequenced (*18–20*). These IGFBPs are produced locally by most tissues, including many tumors (*21–23*). They are present in the blood, extracellular fluids, and cell culture media and can inhibit or augment the actions of IGF at the membrane receptor level.

All 3 components of the IGF system are involved in the initiation, growth, and regulation of various tumors. Hence, methods to diagnose or treat tumors could be developed by altering any part of this complicated loop. In a previous study, we investigated the possibility of using a radiolabeled des(1–3)IGF-I (a truncated IGF-I) to detect tumors in nude mice bearing a tumor xenograft (*24*). In the present investigation, we evaluated the biodistribution of ^{125}I-labeled IGF-I in nude mice bearing NWTc43 tumor xenografts, which overexpress IGF receptors. The radiolabeled IGF-I was incubated in serum and plasma from rats and nude mice to define any difference in binding to the IGFBPs as well as differences between the 2 species. The samples were ana-

Received Aug. 4, 1998; revision accepted May 25, 1999.

For correspondence or reprints contact: Jorge A. Carrasquillo, MD, Bldg. 10, Rm. 1C496, National Institutes of Health, 10 Center Dr., MSC 1180, Bethesda, MD 20892-1180.

lyzed by size-exclusion chromatography. Formation of complexes of IGF-I and IGFBPs in serum samples obtained in vivo was also studied by high-performance liquid chromatography (HPLC). The internalization and catabolism of ^{125}I-labeled IGF-I also was studied by in vitro incubation with tumor cells.

MATERIALS AND METHODS

Cell Line and IGF Ligand

The NWTc43 cell line (a National Institutes of Health (NIH)-3T3 mouse fibroblast) was used for in vivo and in vitro studies. This cell line was genetically engineered by transfecting NIH-3T3 cells with a cDNA insert that encodes the IGF-IR gene (*25*). The cells were routinely maintained in Dulbecco's modified Eagle's medium (DMEM) (Biofluids Inc., Rockville, MD) supplemented with 10% fetal bovine serum, 100 U/mL penicillin, 100 μg/mL streptomycin, 2 mmol/L glutamine, and 500 μg/mL G418 (GIBCO, Grand Island, NY) in a humidified atmosphere of 95% air and 5% CO_2 at 37°C. Human recombinant IGF-I (receptor grade) was purchased from GroPep Pty. Ltd. (Adelaide, Australia).

Radioiodination of Growth Peptide

The IGF-I was labeled with carrier-free Na^{125}I (Amersham, Arlington Heights, IL) by the chloramine-T method (*24*). These radiolabeled ligands were purified by elution through a human serum albumin (HSA)-treated PD-10 column (Pharmacia Biotech AB, Uppsala, Sweden). The specific activity of ^{125}I-labeled IGF-I was 2.22–3.33 GBq/mg. The radiochemical purity of the ligand was >95% as determined by a combination of 2 paper chromatography systems (Whatman 1 paper developed with 85% methanol in 0.05 mol/L phosphate-buffered saline [PBS], pH 6.2; and Whatman 1 paper pretreated with 5% HSA, developed with 0.05 mol/L PBS, pH 6.2) and size-exclusion HPLC, using a TSK G2000SW column (Tosa Haas, Philadelphia, PA; 0.067 mol/L sodium PBS with −0.1 mol/L KCl, pH 6.8, 0.5 mL/min) and an on-line radioactivity detector.

Receptor-Binding Assays

The IGF-I binding to NWTc43 cells was evaluated by competitive receptor-binding assays and saturation-binding assays, as reported previously (*24*). Briefly, NWTc43 cells were seeded in triplicate and cultured overnight in 12-well culture plates with 250,000 cells in each well. Confluent cells were washed with 1 mL binding buffer (0.1 mol/L *N*-[2-hydroxyethl]piperazine-*N'*-[2-ethane sulfonic acid], 0.12 mol/L NaCl, 1.2 mmol/L $MgSO_4$, 2.5 mmol/L KCl, 10 mmol/L glucose, 10 mg/mL radioimmunoassay-grade bovine serum albumin [BSA]; pH 8.0) and incubated in 1 mL binding buffer containing 25,000 cpm (80 pmol) ^{125}I-labeled IGF-I and various concentrations of cold ligands ranging from 1.4×10^{-11} to 10^{-8} mol/L at 4°C for 6 h. After incubation, the cells were washed twice with cold PBS to remove the nonbound activity. The cells were dissolved in 1 mL 0.2 N NaOH and transferred to tubes, and the radioactivity was counted in a γ counter (Packard Auto-Gamma, Meriden, CT). Scatchard analysis was performed using the program LIGAND (*26*).

Saturation-binding studies were performed using radiolabeled IGF-I (0.2–0.25 ng) with cell numbers ranging from 0.25 to 6×10^6 per well, seeded in 6-well plates. After 6 h of incubation at 4°C, the cells were washed, harvested, and counted as described above. The nonspecific binding was evaluated with a 2500-fold excess of cold IGF-I in 1 well.

Catabolism Study

The catabolism of radiolabeled IGF-I by NWTc43 cells was evaluated in vitro, as described elsewhere (*24*). Briefly, 1×10^6 NWTc43 cells per well were seeded and cultured in 6-well culture plates for 12 h. After washing with ice-cold binding buffer, the radiolabeled IGF-I (9.25 kBq, 0.75 nmol/L) was added to the cells in a volume of 0.6 mL and incubated at 4°C for 6 h to allow binding to the receptors. The cells were washed twice with 1 mL cold PBS to remove non–cell-bound activity. The cells (triplicate wells) were diluted with 1 mL DMEM and then incubated at 37 °C or at 4°C for various lengths of time ranging from 0 to 26 h. The culture media were aspirated and saved in test tubes and then assayed further by trichloroacetic acid (TCA) precipitation. The cells were solubilized (dissolved) in 0.2 N NaOH and collected. The radioactivity in the TCA precipitate (containing intact radiolabeled ligands), nonprecipitable supernatant (containing catabolic products), and cell lysates was measured in a well γ counter.

IGF-I Binding to IGFBPs In Vitro

To evaluate the binding of the peptide to IGFBPs and to determine the appropriate amounts of unlabeled IGF-I for use in the saturation study in tumor-bearing nude mice, ^{125}I-labeled IGF-I was incubated in serum and analyzed by HPLC. Radiolabeled IGF-I (1.5 ng, 100,000 cpm) was mixed with unlabeled ligand in a volume of 10 μL and added to 100 μL serum (prewarmed to 37°C) to reach final concentrations of 13–6830 ng/mL serum. The serum samples were incubated at 37°C for 15 min and applied immediately to a TSK G2000SW column, equipped with an on-line NaI γ detector (Gamma RAM, IN/US Systems, Inc., Pine Brook, NJ). The column then was eluted with 0.067 mol/L sodium PBS and 0.1 mol/L KCl, pH 6.8 (0.5 mL/min). Markers of known molecular weight (M_r) were used to calibrate the column: vitamin B_{12} (M_r, 1,350), equine myoglobin (M_r, 17,000), chicken ovalbumin (M_r, 44,000), bovine gamma globulin (M_r, 158,000), and thyroglobulin (M_r, 670,000) (Bio-Rad Laboratories, Hercules, CA).

Previous studies characterizing the effect of IGFBPs have used either serum or plasma, predominantly in rats, and have not characterized well the differences related to these parameters. To assess the possible difference in binding to the IGFBPs in serum and plasma, as well as among animal species, and to allow comparisons with other studies in the literature, radiolabeled IGF-I was incubated in freshly prepared serum and plasma from rats and nude mice and analyzed by HPLC. For preparation of the serum, blood samples from normal rats or nude mice were collected by cardiac puncture after the animals had been killed by CO_2 inhalation. These samples were allowed to clot at room temperature for 15 min and then were centrifuged at 2000 rpm for 5 min. Two methods were used to prepare plasma samples. After blood was drawn by syringe, it was immediately transferred to sterile tubes pretreated with heparin or acid citrate dextrose (ACD). The samples were kept at room temperature for 30 min and then centrifuged. Ten microliters radiolabeled IGF-I (with a final concentration of 50 ng/mL) were incubated with 100 μL serum or plasma at 37°C for 15 min and then analyzed by HPLC. To explore further the effect of heparin on IGF-I and IGFBPs, separate serum samples were mixed with different concentrations of heparin and labeled ^{125}I-labeled IGF-I. These mixtures were incubated and analyzed as described. A mixture of heparin and IGF-I was also incubated in PBS and studied by HPLC.

IGF-I Binding to IGFBPs In Vivo

To determine the degree of binding of IGF-I to the IGFBPs in the circulation, sera from nude mice were analyzed by size-exclusion HPLC after intravenous administration of radiolabeled IGF-I. Five groups of 3 mice each were injected intravenously with 152–163 kBq radiolabeled IGF-I in 100 μL PBS. Blood samples were collected by cardiac puncture from each mouse at 15, 45, 90, 180, and 360 min after injection. Serum was separated by centrifugation from the clotted blood. A volume of 100–150 μL of serum was added to an HPLC with a TSK G2000 column that was eluted with 0.067 mol/L sodium PBS and 0.1 mol/L KCl, pH 6.8, at 0.5 mL/min. The elution profile was measured with an on-line radioactivity detector. The percentage injected dose per gram (%ID/g) of blood was determined, and the components of radioactivity that were associated with ligand–IGFBP complex, intact ligand, and catabolites were quantitated.

Serum samples from other groups of mice (n = 3 mice) that were coinjected with carrier-added ^{125}I-labeled IGF-I were also analyzed by HPLC at 90 min after injection. The procedures for serum preparation and HPLC analysis were the same as described.

Urine samples also were collected from mice at various times after injection with radiolabeled IGF-I. These samples were analyzed by HPLC.

Biodistribution Study

All animal studies were approved by the Animal Care and Use Committee of the Clinical Center at NIH. Biodistribution studies were performed on nude mice bearing NWTc43 tumor xenografts. Female athymic nude mice (nu/nu), 4–6 wk old and weighing 15–20 g, were obtained from Harlan-Sprague-Dawley (Frederick, MD). The mice were inoculated subcutaneously in the right thigh with 1×10^7 (100 μL) NWTc43 cells. Experiments were performed approximately 5 wk later, when the tumors weighed 1.0–2.0 g. Before injection, the purified, radiolabeled IGF-I product was diluted with 0.1 mol/L PBS (pH, 7.4; 1% BSA) and filtered through a 0.22-μm filter (Millipore, Bedford, MA). Three groups of 5 tumor-bearing nude mice were injected intravenously with 0.15–0.16 MBq/100 μL ^{125}I-labeled IGF-I (33–44 ng/20 g body weight) through the tail vein. At 15, 45, and 90 min after injection, the animals were killed by CO_2 inhalation and exsanguinated by cardiac puncture. Organs were removed and weighed, and the radioactivity was counted in a well γ counter. The radioactivity in organs was expressed as %ID/g tissue and normalized to a body weight of 20 g. At the time of the biodistribution studies, the mice weight ranged from 20.5 to 29.3 g (mean ± SD, 25.2 ± 2.5 g).

We evaluated the effect of cold carrier on the biodistribution of radiolabeled IGF-I in normal tissues as well as in tumor tissue. Five tumor-bearing nude mice were injected with a mixture of ^{125}I-labeled IGF-I (167–181 kBq) and a 50-fold excess of unlabeled IGF-I (2200–2800 ng/20 g). Mice were killed at 90 min after injection. The uptake of ^{125}I-labeled IGF-I by normal organs and by the tumor was determined. The biodistribution data were compared with data from the mice that received the radiolabeled ligand alone.

Statistics

Nonpaired Student *t* tests were performed to compare the mean values from the carrier-free and carrier-added groups. Probability values ≤ 0.05 were considered statistically significant.

RESULTS

Receptor-Binding Assays

A range of 7.5–7.7 × 10^5 receptor sites per cell was found in the NWTc43 cell line, based on the competitive receptor binding assay. The K_d for IGF-I with NWTc43 cells was 7.1–7.9 × 10^{-10} mol/L. The maximum binding of radiolabeled IGF-I to NWTc43 was 70%–75% as calculated from the saturation binding assays.

Catabolism Study

Table 1 shows the catabolism of radiolabeled IGF-I by NWTc43 cells incubated at 37°C or at 4°C for up to 26 h. Initially, when the cells were incubated at 37°C, most of the radioactivity was bound to the cells. This cell-bound activity fell very rapidly to only 38% at 90 min and to 5% at 26 h. However, the radioactivity in the catabolite fraction (TCA-soluble) continuously increased, suggesting that the IGF-I was quickly catabolized by the NWTc43 cells, thereby releasing the catabolites into the medium. The TCA-precipitable fraction (intact ligand) reached 31% at 3 h. Its retention was much higher than that of ^{125}I-labeled des-IGF-I (*24*). Its more rapid release from the cell-bound fraction suggests that IGF-I was released from the cell and possibly bound to the IGFBPs in the FBS used in the culture medium.

TABLE 1
Catabolism of ^{125}I-Labeled IGF-I by NWTc43 Cells In Vitro Incubation at 37°C and 4°C

Time (h)	37°C			4°C		
	TCA-precipitable	TCA-soluble	Cell-bound	TCA-precipitable	TCA-soluble	Cell-bound
0	2.0 ± 0.8	0.7 ± 0.2	97.4 ± 1.0	2.0 ± 0.8	0.7 ± 0.2	97.4 ± 1.0
0.25	10.8 ± 0.5	3.3 ± 0.3	85.9 ± 0.5	8.7 ± 0.5	2.2 ± 0.2	89.1 ± 0.7
0.75	21.6 ± 0.6	13.5 ± 1.1	64.8 ± 1.6	9.7 ± 0.5	2.4 ± 0.2	87.8 ± 0.7
1.5	29.6 ± 0.7	32.0 ± 1.5	38.4 ± 1.9	9.7 ± 0.4	2.3 ± 0.2	88.1 ± 0.6
3.0	31.2 ± 1.0	54.0 ± 0.4	14.8 ± 0.6	13.6 ± 1.0	2.7 ± 0.1	83.7 ± 1.1
6.0	29.0 ± 0.5	63.4 ± 0.3	7.5 ± 0.8	19.1 ± 1.1	3.9 ± 0.2	77.0 ± 1.0
18	23.7 ± 0.4	71.6 ± 0.6	4.8 ± 0.3	34.6 ± 1.5	4.4 ± 0.1	61.0 ± 1.4
26	19.9 ± 0.2	75.0 ± 0.2	5.1 ± 0.4	39.6 ± 0.7	6.8 ± 0.3	53.6 ± 0.9

Data are expressed as percentage of total activity recovered from 3 fractions (mean ± SD, n = 3 per point).

When cells were incubated at 4°C, most of the radiolabeled IGF-I remained cell-bound, either on cell surfaces or internalized (Table 1). This cell-bound activity was released more slowly into the culture medium at 4°C than at 37°C. In addition, the greater part of the activity released into the culture medium was TCA precipitable, indicating that the radiolabeled ligands were not catabolized as quickly at 4°C as at 37°C. The catabolite fraction was much lower at 4°C than at 37°C.

IGF-I Binding to IGFBPs In Vitro

Radiolabeled IGF-I was incubated in vitro in nude mouse serum at different specific activities to evaluate its binding to the IGFBPs. The sera were incubated with radiolabeled IGF-I and various concentrations of unlabeled peptide and analyzed by size-exclusion HPLC. Two complex peaks of different molecular weights were observed: 1 at approximately 150 kDa and another at 30 to 50 kDa (Fig. 1). The formation of ligand–IGFBP complexes was not seen when the concentration of ligand was >1000 ng/mL. However, as the ligand concentration was reduced, the complexes quickly increased from 13% at 580 ng/mL to 76% at 13 ng/mL, whereas free IGF-I decreased from 79% to 20% (Fig. 1).

The binding of IGF-I to the IGFBPs in serum and plasma was studied in vitro by HPLC (Fig. 2). In nude mouse serum, the radioactivity was mainly associated with the peak of 30 to 50 kDa, which in turn was composed of 2 smaller peaks (Fig. 2A). The ACD-prepared plasma had a binding pattern identical to that of the serum (Fig. 2B). However, in heparinized plasma, the 150-kDa complex became dominant (Fig. 2C), leaving a smaller 30- to 50-kDa peak and an increased intact IGF-I peak, each larger than those of the serum and ACD-prepared plasma samples. We then evaluated the relationships among heparin, IGF-I, and IGFBP by mixing serum with various amounts of heparin. Interestingly, the serum then showed a radioactivity-distribution pattern similar to that observed with the heparinized plasma,

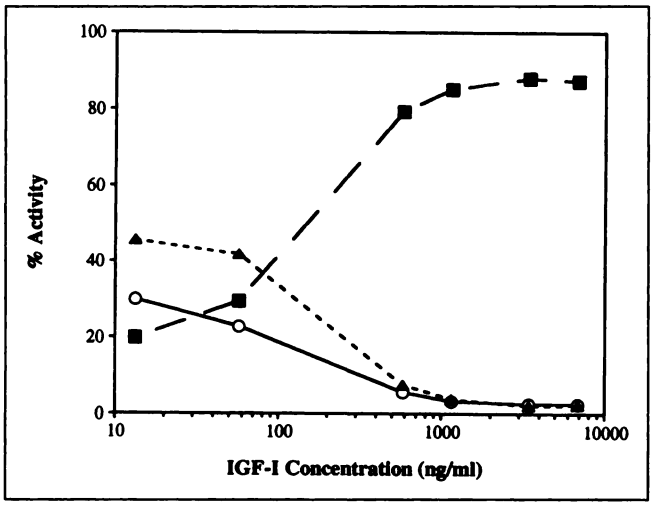

FIGURE 1. HPLC analysis of nude mouse sera incubated in vitro with ^{125}I-labeled IGF-I (1.5 ng) in presence of increasing amounts of unlabeled IGF-I. Percentages of radioactivity present in high-molecular-weight (150-kDa) complex (○), in low-molecular weight (30–50 kDa) complex (▲), and as free IGF-I fraction (■) are shown. IGF-I concentrations represent combined total of radiolabeled ligand plus unlabeled ligand as represented by the ^{125}I-label.

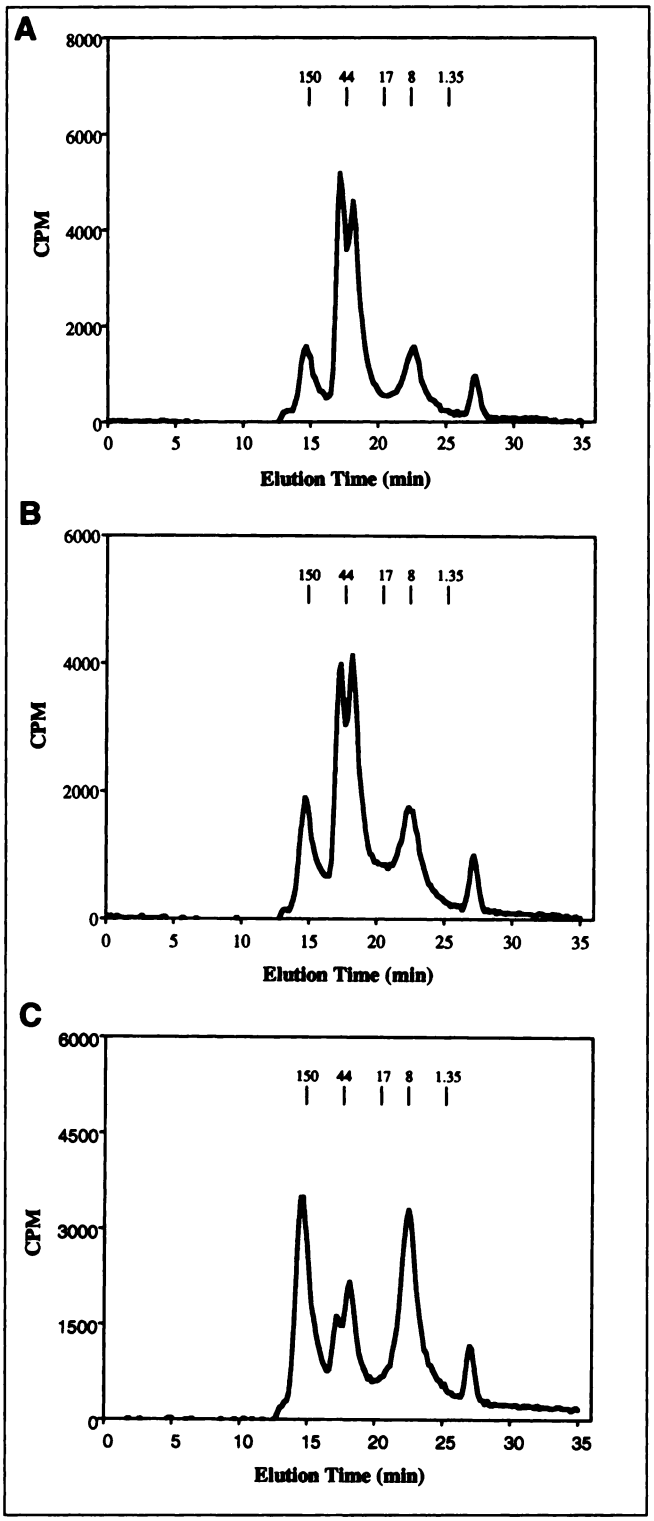

FIGURE 2. Radiolabeled IGF-I (final concentration, 50 ng/mL) was incubated in nude mouse serum (A), ACD-prepared plasma (B), or heparinized plasma (C) at 37°C for 15 min and analyzed by HPLC.

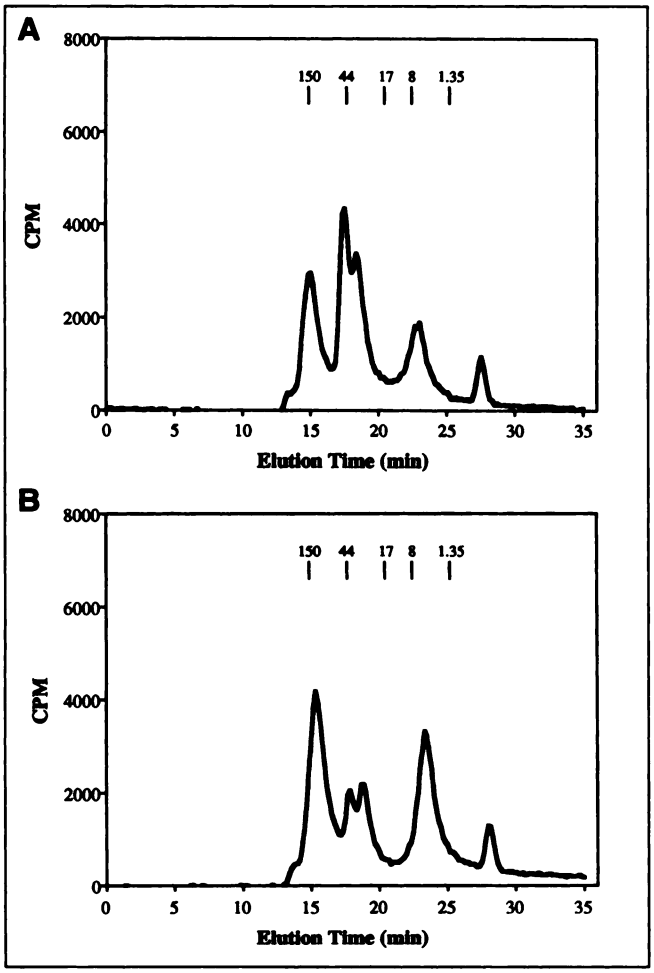

FIGURE 3. HPLC profiles of nude mouse serum incubated at 37°C for 15 min with mixture of heparin and radiolabeled IGF-I (final concentration, 50 ng/mL). (A) 4.5 U/mL heparin. (B) 45 U/mL heparin.

i.e., a shift of radioactivity from the 30- to 50-kDa peak to the 150-kDa peak and to the intact IGF-I peak in a dose-dependent manner (Fig. 3). When mixing the heparin and radiolabeled IGF-I in PBS, we observed only 1 intact IGF-I peak and no evidence of binding of heparin to IGF-I.

The differences in binding properties of IGF-I to IGFBPs between species were evaluated with serum and plasma samples from nude mice and rats. In mouse serum samples, 82% of radiolabeled IGF-I was associated with a 30- to 50-kDa complex, whereas in rat serum only 21% appeared in this complex (Table 2). In rat serum, more than 50% of radioactivity was found associated with intact free ligand compared with only 7% for mouse serum, indicating much less binding of IGF-I to IGFBPs in rat serum. In the plasma, the shifting of radioactivity from the smaller to the larger complex was seen in both mice and rats. Considerable amounts of activity also appeared in the free IGF-I peak in mouse plasma. However, the percentage of radioactivity in the intact IGF-I peak of rat plasma did not differ much from that of rat serum (Table 2).

IGF-I Binding to IGFBPs In Vivo

To study the binding of circulating ligands to the IGFBPs in vivo, size-exclusion chromatography of mouse serum was performed after the injection of radiolabeled IGF-I. Nude mice were injected intravenously with radiolabeled ligand, blood was drawn at 15, 45, 90, 180, and 360 min, and sera were prepared. The results (Table 3) indicate that radiolabeled IGF-I was either bound to IGFBPs in the circulation or catabolized to smaller-molecular-weight ^{125}I-labeled products (less than 1 kDa). There was no activity at the position of labeled IGF-I. At 15 min, 52% of the activity was associated with the smaller IGF–IGFBP complex, 30–50 kDa. This percentage declined gradually with time to 13% at 6 h. However, the percentage of radioactivity in the 150-kDa peak increased from 35% at 15 min to 53% at 90 min and remained as high as 44% for up to 6 h. A continuous increase in radioactivity in the small-molecular-weight catabolites was observed, from 12% at 15 min to 43% at 6 h.

The amount of radioactivity associated with different molecular weight peaks is shown in Table 3. As the blood level decreased with time, the radioactivity in complex 2 (30–50 kDa) also quickly diminished. However, the activity in complex 1 (150 kDa) was nearly constant from 15 to 90 min but then decreased slowly (Table 3). The activity in the catabolite peak remained unchanged from 15 min to 3 h but declined later because of excretion of the catabolites into the gastrointestinal tract.

To determine the effect of carrier on the binding of IGF-I to the circulating binding proteins, mice were coinjected with the unlabeled ligand, and serum was analyzed by HPLC 90 min after injection. When comparing the serum HPLC profiles from the carrier-free mice with those from the carrier-added mice, remarkable differences were observed in

TABLE 2
HPLC Analysis of ^{125}I-IGF-I Incubated in Serum and Plasma from Mice and Rats

	Serum			Plasma		
Animal	Complex 1 (150 kDa)	Complex 2 (30–50 kDa)	IGF-I	Complex 1 (150 kDa)	Complex 2 (30–50 kDa)	IGF-I
Mouse	10.30 ± 1.29	81.91 ± 2.40	6.70 ± 0.65	38.82 ± 1.12	34.69 ± 3.36	23.93 ± 4.32
Rat	25.00 ± 0.03	21.49 ± 0.24	51.50 ± 0.70	42.02 ± 0.51	11.57 ± 0.05	43.71 ± 0.80

Data are expressed as percentage of radioactivity in each elution fraction (mean ± SD; n = 2 animals per group).

TABLE 3
HPLC Analysis of Nude Mouse Serum After Injection of ^{125}I-Labeled IGF-I

Time (min)	% Activity* Complex 1 (150 kDa)	% Activity* Complex 2 (30–50 kDa)	% Activity* Catabolite	%ID/g† Complex 1 (150 kDa)	%ID/g† Complex 2 (30–50 kDa)	%ID/g† Catabolite
15	35.1 ± 4.6	51.7 ± 3.3	11.5 ± 1.2	6.5 ± 0.9	9.6 ± 0.6	2.1 ± 0.2
45	46.5 ± 3.5	33.6 ± 1.7	19.1 ± 2.2	6.2 ± 0.5	4.5 ± 0.2	2.6 ± 0.3
90	53.3 ± 7.1	26.1 ± 2.8	20.3 ± 7.1	6.1 ± 0.1	3.0 ± 0.5	2.4 ± 1.2
180	43.3 ± 2.2	21.4 ± 2.7	35.1 ± 3.9	3.3 ± 0.7	1.6 ± 0.3	2.7 ± 1.1
360	44.3 ± 0.6	13.0 ± 2.1	42.7 ± 2.7	1.7 ± 0.1	0.5 ± 0.1	1.6 ± 0.0

*Data are expressed as percentage of radioactivity in each elution fraction (mean ± SD, n = 3 mice per group).
†Data are expressed as %ID/g serum normalized to body weight of 20 g. Sum of 3 fractions is equal to total activity in serum.

the percentage of radioactivity associated with the 3 peaks (Fig. 4). The radioactivity in complexes 1 and 2 was lower in carrier-added mice (27% and 19%, respectively) than in carrier-free mice (53% and 26%, respectively), reflecting the partial saturation of binding sites in the carrier-added mice. The unbound IGF-I was catabolized in the kidneys, and the catabolic products were quickly released back into the circulation, producing a considerable rise in the catabolite peak to 53% for carrier-added mice versus 20% for carrier-free mice.

To assess the excretion of radiolabeled ligands, urine samples were collected and analyzed by HPLC. The urine HPLC profile showed only 1 catabolite peak at all time points, suggesting that the radiolabeled ligands were completely metabolized in vivo (data not shown). Nevertheless, because of limitations in resolution, this method does not allow a determination of how many different catabolite products were present. The metabolites were either expelled into urine or released back into the circulation and eventually excreted into the gastrointestinal tract.

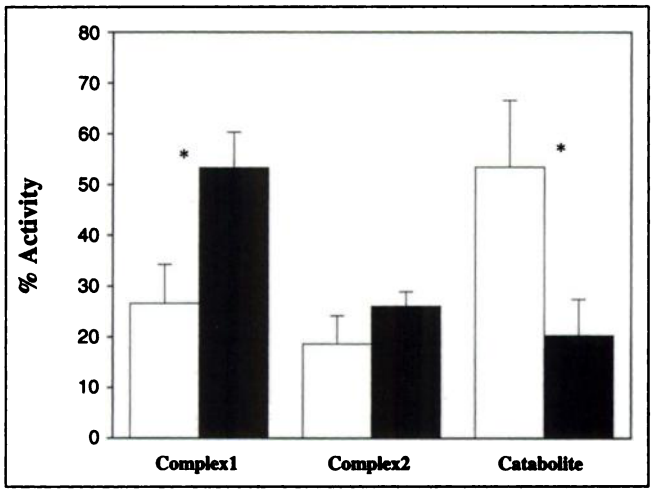

FIGURE 4. Size-exclusion HPLC analysis of nude mouse serum after injection of radiolabeled IGF-I with unlabeled ligand (white bars) or without unlabeled ligand (black bars). Serum was prepared 90 min after injection. Data are expressed as percentage of radioactivity associated with fractions of complex 1, complex 2, and catabolites (mean ± SD; n = 3; *$P < 0.05$).

Biodistribution Study

Table 4 summarizes the biodistribution results of radiolabeled IGF-I in tumor-bearing nude mice. In the carrier-free mice, the highest uptake of radioactivity in all the normal tissues occurred 15 min after injection and then decreased with time, except in the stomach, where it doubled with time. The kidneys showed a much faster clearance than other tissues. The tumor uptake decreased with time.

To determine the effect of carrier on the biodistribution of the IGF-I, tumor-bearing nude mice received a coinfusion of radiolabeled IGF-I and homologous unlabeled ligand. The radioactivity uptake in most of the normal tissues was lower in the carrier-added mice than in the carrier-free mice (Table 4). The tumor uptake in carrier-added mice was significantly higher than that in carrier-free mice ($P <$

TABLE 4
Biodistribution of ^{125}I-Labeled IGF-I in NWTc43 Tumor-Bearing Nude Mice

Organ	15 min after injection; carrier (−)	45 min after injection; carrier (−)	90 min after injection Carrier (−)	90 min after injection Carrier (+)
Blood	18.3 ± 0.6	13.3 ± 0.2	10.7 ± 1.8	6.4 ± 1.1*
Kidney	60.3 ± 6.0	17.3 ± 2.4	8.9 ± 1.7	7.3 ± 1.6
Liver	11.4 ± 1.5	6.1 ± 0.3	4.2 ± 0.5	3.1 ± 0.6†
Spleen	7.1 ± 0.9	4.7 ± 0.2	3.4 ± 0.7	3.1 ± 0.6
Stomach	15.3 ± 3.3	24.1 ± 5.1	32.1 ± 7.7	43.6 ± 9.5
Intestine	6.8 ± 0.7	4.9 ± 0.3	3.2 ± 0.6	2.7 ± 0.5
Bone	3.8 ± 0.4	2.9 ± 0.2	2.3 ± 0.4	2.8 ± 0.5
Thyroid	9.5 ± 0.8	9.0 ± 1.8	7.0 ± 1.5	8.6 ± 3.9
Heart	7.7 ± 0.5	5.8 ± 0.4	4.8 ± 1.0	3.4 ± 0.7†
Lung	13.6 ± 1.0	9.7 ± 0.7	6.6 ± 1.1	6.0 ± 1.8
Tumor	6.5 ± 0.7	5.9 ± 0.5	3.9 ± 0.8	7.6 ± 1.7‡

*$P < 0.0001$.
†$P < 0.05$.
‡$P < 0.005$.
Radioactivity was expressed as %ID/g tissue (mean ± SD, n = 5 mice per group).

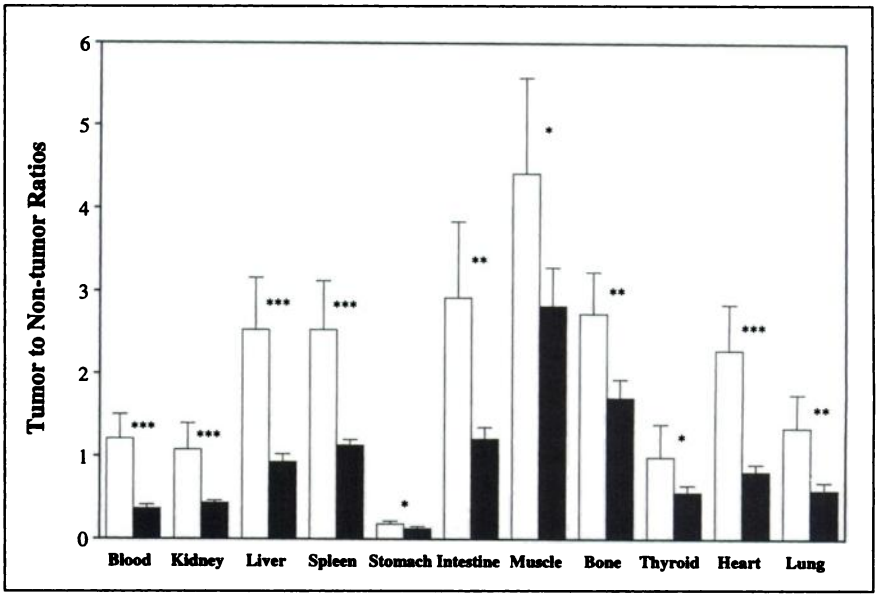

FIGURE 5. Tumor-to-normal tissue ratios in nude mice bearing NWTc43 tumor xenografts after injection of radiolabeled IGF-I with (black bars) or without (white bars) unlabeled peptides. Animals were killed 90 min after injection (mean ± SD; n = 5; $^*P < 0.05$, $^{**}P < 0.01$, $^{***}P < 0.0001$).

0.005), resulting in significantly higher tumor-to-normal tissue ratios (Fig. 5).

DISCUSSION

The use of radiolabeled IGF-I for tumor imaging is influenced by many factors. The action of IGF-I is modulated through its interaction with its receptors on the membrane of target cells. The existence of IGFBPs in the circulation complicates this situation. By binding to the IGFBPs, less free IGF-I is available for its receptors, and this contributes to a high background, because the complexes stay in the circulation longer than the free ligand. To deal with this problem, 3 approaches have been considered: using des-IGF-I, which showed low affinity for IGFBPs; saturating the binding sites of IGFBPs with unlabeled peptide; and blocking the IGF-IGFBP complex formation with other reagents. We reported our results with the first approach elsewhere (*24*). The second approach is discussed extensively in this article, whereas the last approach was addressed only in vitro.

Avid binding of IGF-I to the IGFBPs has been well documented (*27–30*), whereas des(1–3)IGF-I showed very little binding to the IGFBPs in vitro (*24*). The marked binding of IGF-I was observed in our current experiments both in vitro and in vivo. The amount of radioactivity associated with the 150-kDa and 30- to 50-kDa complexes was different in serum from that in heparinized plasma. In serum, more labeled IGF-I was bound to the IGFBPs, and this was primarily associated with 30- to 50-kDa complexes. In heparinized plasma, the activity that appeared in the small-complex peak was low; correspondingly, the intact free-ligand peak was increased, as was the 150-kDa complex peak. This change was not found in ACD-prepared plasma, which gave a pattern of radioactivity distribution essentially identical to that seen in serum samples, suggesting that the binding to IGFBPs in the heparinized plasma was reduced. Reports have shown that all forms of IGFBPs, except for IGFBP-4, have at least 1 putative heparin-binding domain (*31–33*). Heparin binding to these regions resulted in a conformational change in IGFBPs, which lowered their affinity for IGF-I. This was also confirmed by our results. When the heparin was added to serum, we observed a binding pattern resembling that of heparinized plasma (Fig. 3). The binding of heparin with IGFBPs could improve tumor targeting using IGF-I. Obviously, the formation of IGF–IGFBP complexes lowers the amount of free IGF-I for its cellular receptors. Therefore, partial or complete blocking of IGF–IGFBP complex formation with heparin or heparin-like glycosaminoglycans, such as heparan sulfate, dermatan sulfate, dextran sulfate, or pentosan polysulfate, could improve tumor targeting (*34–37*). Animal studies in the literature have often failed to address the issue of the effect of heparinized plasma.

Species differences in the binding of IGF-I to IGFBPs have been reported (*38*). We also found this in our experiments with serum and plasma samples from nude mice and rats (Table 2). The uncomplexed IGF-I was much higher in rat serum than in mouse serum, suggesting a lower binding capacity in the rat. In the mouse, heparin inhibited IGF-I binding by markedly reducing the radioligands in the 30- to 50-kDa complex and increasing the percentage of free ligand in the 150-kDa complex. Although heparin lowered the radioactivity associated with the small complex in the rat, the radioligands shifted to the larger complex, but the percentage of free ligand remained unchanged.

The saturation of the binding sites of IGFBPs with unlabeled ligand subsequently lowered the formation of complexes, both in vitro and in vivo. Our in vitro studies revealed a remarkable shift of radiolabeled IGF-I from the free form to the complexed form as the concentrations of unlabeled IGF-I in the serum decreased, suggesting saturation of the binding sites within IGFBPs. At the lowest

concentration, almost 80% of the radioactivity was found in IGF-I–IGFBP complexes (Fig. 1), whereas at the higher concentration, almost all the radiolabeled IGF-I was free, available for binding to its cellular receptors. If clinical imaging studies are performed with any radiolabeled IGF reagent, the issue of dose dependency on biodistribution will need to be addressed.

For in vivo studies, we saturated the binding sites of IGFBPs in the circulation with coinjections of radiolabeled and unlabeled IGF-I. With an excess of cold peptides, the formation of IGF-I–IGFBP complexes in the serum was inhibited as a result of the saturation of IGFBPs by the unlabeled ligands. Although the HPLC profiles did not show a free IGF-I peak, the higher catabolite fraction observed in carrier-added mice suggested that more radiolabeled IGF-I was metabolized in these mice by tumor or by other tissues, because only free ligands could bind to the receptors. These catabolites were quickly excreted into the urine or gastrointestinal tract. This was confirmed by the higher stomach uptake of radioactivity in carrier-added mice compared with carrier-free mice. Added carrier hastened the clearance of ^{125}I-labeled IGF-I from the blood and lowered nonspecific uptake in other organs (Table 4). At the same time, tumor uptake in carrier-added mice was increased because of the greater availability of free ^{125}I-labeled IGF-I, resulting in better tumor-to-nontumor ratios (Fig. 5). We previously observed a similar improvement in tumor-to-nontumor concentration ratios with ^{125}I-labeled des-IGF-I (*24*).

An in vitro endocytosis assay showed the internalization of IGF-I receptors after the binding of ^{125}I-labeled IGF-I. This was also observed by other investigators (*39–40*) and in our previous study with des-IGF-I (*24*). As the incubation time approached 26 h, the radioactivity associated with the TCA-soluble proportion continuously increased, indicating the catabolism of endocytosed IGF-I by the cells. Similar catabolism likely occurred in vivo, consistent with the decrease in tumor uptake and the increase in the circulatory catabolites (Table 3). The high stomach uptake of ^{125}I was presumably iodide (Table 4). Because of its size (7.5 kDa), IGF-I is highly concentrated in renal tubular cells and catabolizes quickly, like most low-molecular-weight proteins. High radioactivity in the stomach was observed from reabsorbed iodide; HPLC analysis of urine samples revealed a single peak with a retention time consistent with iodide.

CONCLUSION

The use of radiolabeled IGF-I for tumor targeting has many potential advantages: many tumors overexpress IGF-IR or IGF-IIR; IGFs are natural, endogenous materials that will not cause adverse effects in humans; immunogenicity will not be a problem because of their small molecular weight; and IGFs penetrate into tumor cells quickly because of their low molecular weight. However, the existence of IGFBPs in serum not only elevates the background activity but also reduces the amount of free IGF-I available for the tumor tissue, resulting in low tumor-to-nontumor ratios. The combination of approaches—using an IGF analog with less affinity for IGFBPs, saturating the binding sites of IGFBPs with unlabeled ligands, and possibly inhibiting IGF binding to IGFBPs with heparinlike glycosaminoglycans or other binding agents—will likely improve tumor localization. Further progress can probably be achieved by developing IGF-I analogs with even less affinity for IGFBPs, such as Long R^{3}IGF-I (*38*), and analogs with slower catabolic rates. The rapid catabolism and loss of the radiolabel from tumors when using ^{125}I-labeled IGF-I is suboptimal. Radiolabeling these analogs with ^{111}In or other radioelements that tend to remain intracellular in tumor cells should also be tried, because these radioelements are not as promptly released from cells as is radioiodide.

ACKNOWLEDGMENTS

The authors thank Drs. Vicky A. Blakesley and Lee J. Helman, National Cancer Institute, National Institutes of Health, Bethesda, MD, for the cell lines and helpful discussions.

REFERENCES

1. Daughaday WH, Rotwein P. Insulin-like growth factors I and II. Peptide, messenger ribonucleic acid and gene structures, serum, and tissue concentrations. *Endocrinol Rev.* 1989;10:68–91.
2. LeRoith D, Roberts CT Jr. Insulin-like growth factors and their receptors in normal physiology and pathological states. *J Pediatr Endocrinol.* 1993;6:251–255.
3. Hana V, Murphy LJ. Expression of insulin-like growth factors and their binding proteins in the estrogen responsive Ishikawa human endometrial cancer cell line. *Endocrinology.* 1994;135:2511–2516.
4. Fleming MG, Howe SF, Graf LH Jr. Expression of insulin-like growth factor I (IGF-I) in nevi and melanomas. *Am J Dermatopathol.* 1994;16:383–391.
5. Lowe WL Jr. Biological actions of the insulin-like growth factors. In: LeRoith D, ed. *Insulin-like Growth Factors: Molecular and Cellular Aspects.* Boca Raton, FL: CRC; 1991:49–85.
6. Teruel T, Valverde AM, Alvarez A, Benito M, Lorenzo M. Differentiation of rat brown adipocytes during late foetal development: role of insulin-like growth factor I. *Biochem J.* 1995;310:771–776.
7. Hernandez-Sanchez C, Lopez-Carranza A, Alarcon C, de La Rosa EJ, de Pablo F. Autocrine/paracrine role of insulin-related growth factors in neurogenesis: local expression and effects on cell proliferation and differentiation in retina. *Proc Natl Acad Sci USA.* 1995;92:9834–9838.
8. Birnbaum RS, Bowsher RR, Wiren KM. Changes in IGF-I and -II expression and secretion during the proliferation and differentiation of normal rat osteoblasts. *J Endocrinol.* 1995;144:251–259.
9. Pretzer D, Ghaida JA, Rune GM. Growth factors (EGF, IGF-I) modulate the morphological differentiation of adult marmoset (*Callithrix jacchus*) Sertoli cells in vitro. *J Androl.* 1994;15:398–409.
10. Ma ZQ, Santagati S, Patrone C, Pollio G, Vegeto E, Maggi A. Insulin-like growth factors activate estrogen receptors to control the growth and differentiation of the human neuroblastoma cell line SK-ER3. *Mol Endocrinol.* 1994;8:910–918.
11. Favoni RE, de Cupis A, Ravera F, et al. Expression and function of the insulin-like growth factor I system in human non-small-cell lung cancer and normal lung cell lines. *Int J Cancer.* 1994;56:858–866.
12. Singh P, Rubin N. Insulin-like growth factors and binding proteins in colon cancer. *Gastroenterology.* 1993;105:1218–1237.
13. Yballe CM, Vu TH, Hoffman AR. Imprinting and expression of insulin-like growth factor-II and H19 in normal breast tissue and breast tumor. *J Clin Endocrinol Metab.* 1996;81:1607–1612.
14. LeRoith D, Werner H, Neuenschwander S, Kalebic T, Helman LJ. The role of the insulin-like growth factor-I receptor in cancer. *Ann N Y Acad Sci.* 1995;766:402–408.
15. Moody TW, Cuttitta F. Growth factor and peptide receptors in small cell lung cancer. *Life Sci.* 1993;52:1161–1173.
16. Quinn KA, Treston AM, Unsworth EJ, et al. Insulin-like growth factor expression in human cancer cell lines. *J Biol Chem.* 1996;271:11477–11483.

17. Nakahashi K, Kitahori Y, Konishi N, Ohnishi T, Sugimura M, Hiasa Y. Establishment of a rat thyroid carcinoma cell line in vitro demonstrating high DNA synthesis in response to insulin-like growth factor I. *Cancer Lett.* 1996;101:247–255.
18. Shimasaki S, Shimonaka M, Zhang HP, Ling N. Identification of five different insulin-like growth factor binding proteins (IGFBPs) from adult rat serum and molecular cloning of a novel IGFBP-5 in rat and human. *J Biol Chem.* 1991;266:10646–10653.
19. Rechler MM. Insulin-like growth factor binding proteins. *Vitam Horm.* 1993;47:1–114.
20. Sheikh MS, Shao ZM, Clemmons DR, LeRoith D, Roberts CT Jr, Fontana JA. Identification of the insulin-like growth factor binding proteins 5 and 6 (IGFBP-5 and 6) in human breast cancer cells. *Biochem Biophys Res Commun.* 1992;183:1003–1010.
21. Shemer J, Yaron A, Werner H, et al. Regulation of insulin-like growth factor (IGF) binding protein-5 in the T47D human breast carcinoma cell line by IGF-I and retinoic acid. *J Clin Endocrinol Metab.* 1993;77:1246–1250.
22. Sheikh MS, Shao ZM, Hussain A, et al. Regulation of insulin-like growth factor-binding-protein-1, 2, 3, 4, 5, and 6: synthesis, secretion, and gene expression in estrogen receptor-negative human breast carcinoma cells. *J Cell Physiol.* 1993;155:556–567.
23. Shao ZM, Sheikh MS, Ordonez JV, et al. IGFBP-3 gene expression and estrogen receptor status in human breast carcinoma. *Cancer Res.* 1992;52:5100–5103.
24. Sun B-F, Kobayashi H, Le N, et al. Biodistribution of ^{125}I-labeled des(1–3)IGF-I in tumor-bearing nude mice and its in vitro catabolism. *Cancer Res.* 1997;57:2754–2759.
25. Blakesley VA, Kalebic T, Helman LJ, et al. Tumorigenic and mitogenic capacities are reduced in transfected fibroblasts expressing mutant insulin-like growth factor (IGF)-I receptors: the role of tyrosine residues 1250, 1251, and 1316 in the carboxy-terminus of the IGF-I receptor. *Endocrinology.* 1996;137:410–417.
26. Munson PJ, Rodbard D. LIGAND: a versatile computerized approach for characterization of ligand-binding systems. *Ann Biochem.* 1980;107:220–239.
27. Szabo L, Mottershead DG, Ballard FJ, Wallace JC. The bovine insulin-like growth factor (IGF) binding protein purified from conditioned medium requires the N-terminal tripeptide in IGF-I for binding. *Biochem Biophys Res Commun.* 1988;151:207–214.
28. Ross M, Francis GL, Szabo L, Wallace JC, Ballard FJ. Insulin-like growth factor (IGF)-binding proteins inhibit the biological activities of IGF-I and IGF-2 but not des-(1–3). *Biochem J.* 1989;258:267–272.
29. Ballard FJ, Knowles SE, Walton PE, et al. Plasma clearance and tissue distribution of labelled insulin-like growth factor-I (IGF-I), IGF-II and des(1–3)IGF-I in rats. *J Endocrinol.* 1991;128:197–204.
30. Lord APD, Martin AA, Ballard FJ, Read LC. Transfer of insulin-like growth factor (IGF)-I from blood to intestine: comparison with IGFs that bind poorly to IGF-binding proteins. *J Endocrinol.* 1994;141:505–515.
31. Cardin AD, Weintraub HJ. Molecular modeling of protein-glycosaminoglycan interactions. *Arteriosclerosis.* 1989;9:21–32.
32. Clemmons DR, Underwood LE, Chatelain PG, Van Wyk JJ. Liberation of immunoreactive somatomedin-C from its binding proteins by proteolytic enzymes and heparin. *J Clin Endocrinol Metab.* 1983;56:384–389.
33. Arai T, Clarke J, Parker A, Busby W Jr, Nam T, Clemmons DR. Substitution of specific amino acids in insulin-like growth factor (IGF) binding protein 5 alters heparin binding and its change in affinity for IGF-I response to heparin. *J Biol Chem.* 1996;271:6099–6106.
34. Baxter RC. Glycosaminoglycans inhibit formation of the 140-kDa insulin-like growth factor-binding protein complex. *Biochem J.* 1990;271:773–777.
35. Arai T, Busby W Jr, Clemmons DR. Binding of insulin-like growth factor (IGF) I or II to IGF-binding protein-2 enables it to bind to heparin and extracellular matrix. *Endocrinology.* 1996;137:4571–4575.
36. Booth BA, Boes M, Bar RS. IGFBP-3 proteolysis by plasmin, thrombin, serum: heparin binding, IGF binding, and structure of fragments. *Am J Physiol.* 1996;271:465–470.
37. Arai T, Parker A, Busby W Jr, Clemmons DR. Heparin, heparan sulfate, and dermatan sulfate regulate formation of the insulin-like growth factor-I and insulin-like growth factor-binding protein complexes. *J Biol Chem.* 1994;269:20388–20393.
38. Lord APD, Bastian SEP, Read LC, Walton PE, Ballard FJ. Differences in the association of insulin-like growth factor-I (IGF-I) and IGF-I variants with rat, sheep, pig, human and chicken plasma-binding proteins. *J Endocrinol.* 1994;140:475–482.
39. Prager D, Li HL, Yamasaki H, Melmed S. Human insulin-like growth factor I receptor internalization: role of the juxtamembrane domain. *J Biol Chem.* 1994;269:11934–11937.
40. Zapf A, Hsu D, Olefsky JM. Comparison of the intracellular itineraries of insulin-like growth factor-I and insulin and their receptors in Rat-1 fibroblasts. *Endocrinology.* 1994;134:2445–2452.